Published in final edited form as:
Epilepsia. 2010 August ; 51(8): 1436–1445. doi:10.1111/j.1528-1167.2009.02413.x.

Involvement of the thalamocortical network in TLE with and without mesiotemporal sclerosis

Susanne G. Mueller[*], **Kenneth D. Laxer**[†], **Jerome Barakos**[†], **Ian Cheong**[*], **Daniel Finlay**[*], **Paul Garcia**[‡], **Valerie Cardenas-Nicolson**[*], and **Michael W. Weiner**[*]

[*] Center for Imaging of Neurodegenerative Diseases, San Francisco, California, U.S.A

[†] Pacific Epilepsy Program, California Pacific Medical Center, San Francisco, California, U.S.A

[‡] Department of Neurology, University of California, San Francisco, California, U.S.A

Summary

Purpose—The thalamus plays an important role in seizure propagation in temporal lobe epilepsy (TLE). This study investigated how structural abnormalities in the focus, ipsilateral thalamus and extrafocal cortical structures relate to each other in TLE with mesiotemporal sclerosis (TLE-MTS) and without hippocampal sclerosis (TLE-no).

Methods—T_1 and high-resolution T_2 images were acquired on a 4T magnet in 29 controls, 15 TLE-MTS cases, and 14 TLE-no. Thalamus volumes were obtained by warping a labeled atlas onto each subject's brain. Deformation-based morphometry was used to identify regions of thalamic volume loss and FreeSurfer for cortical thickness measurements. CA1 volumes were obtained from high-resolution T_2 images. Multiple regression analysis and correlation analyses for voxel- and vertex-based analyses were performed in SPM2 and FreeSurfer.

Results—TLE-MTS had bilateral volume loss in the anterior thalamus, which was correlated with CA1 volume and cortical thinning in the mesiotemporal lobe. TLE-no had less severe volume loss in the dorsal lateral nucleus, which was correlated with thinning in the mesiotemporal region but not with extratemporal thinning.

Discussion—The findings suggest that seizure propagation from the presumed epileptogenic focus or regions close to it into the thalamus occurs in TLE-MTS and TLE-no and results in circumscribed neuronal loss in the thalamus. However, seizure spread beyond the thalamus seems not to be responsible for the extensive extratemporal cortical abnormalities in TLE.

Keywords

Extrafocal cortical thinning; Mesiotemporal sclerosis; Thalamus; Temporal lobe epilepsy

Temporal lobe epilepsy (TLE) is the most common form of partial epilepsy. Based on imaging and histopathologic findings, two types of nonlesional TLE are distinguished: TLE with mesiotemporal lobe sclerosis (TLE-MTS) characterized by an atrophied hippocampus with signal abnormalities on magnetic resonance imaging (MRI) and severe neuronal loss on histologic examination (TLE-MTS, about 60–70%), and TLE with normal-appearing hippocampus on MRI and no or only mild hippocampal neuronal loss on histologic examination (TLE-no, about 30–40%). Depth electroencephalography (EEG) recordings (Vossler et al.,

Address correspondence to Susanne G. Mueller, MD, Center for Imaging of Neurodegenerative Diseases, SFVAMC, Clement Street 4150, San Francisco, CA, 94121, U.S.A. susanne.mueller@ucsf.edu.

Disclosure: None of the authors has any conflict of interest to disclose.

2004) and neuroimaging (Carne et al., 2007, Mueller et al., 2007a) suggest that in TLE-MTS seizures arise from a circumscribed region in the mesiotemporal region/hippocampus as opposed to TLE-no, wherein they arise from a more widespread, less well-defined region in inferolateral temporal lobe. In both conditions, seizures are not restricted to the hippocampus and/or temporal lobe, but can also spread to other brain regions and cause structural and metabolic abnormalities similar to those in the focus (Jutila et al., 2001; Moran et al., 2001; Keller et al., 2004).

A structure of particular interest in this regard is the thalamus, in which bilateral volume loss and/or uni- or bilateral hypometabolism have consistently been described in TLE-MTS (Juhasz et al., 1999; Mueller et al., 2006, 2007a; Gong et al., 2008; Labate et al., 2008; Seidenberg et al., 2008). The thalamus not only receives massive neuronal projections from temporal limbic regions but has also widespread reciprocal connections to subcortical structures and other cortical regions. Because of its unique role as gateway between brain structures, it has been suggested that the thalamus might play an active role in seizure propagation to other brain regions (Margerison & Corsellis, 1966; Lothman & Collins, 1981; Cassidy & Gale, 1998; Rosenberg et al., 2006; Guye et al., 2006; Bertram et al., 2008; Sloan & Bertram, 2008). Seizure spread beyond the thalamus could cause neuronal loss due to deafferentation or local excitotoxic effects and thus contribute to the widespread extratemporal structural abnormalities observed in TLE. To our knowledge the relationship between thalamic volume losses and structural changes in extratemporal brain regions in TLE has not been studied systematically. The overall aim of this study was to further investigate how volume losses in the epileptogenic focus (TLE-MTS, hippocampus; TLE-no, cortical: thickness of the inferior temporal gyrus), ipsilateral thalamus, and extrafocal cortical structures relate to each other using the FreeSurfer software package (version 3.05; https://surfer.nmr.mgh.harvard.edu) to assess cortical thickness and deformation-based morphometry to identify regions of thalamic volume loss. Specifically, the following hypotheses were tested: (1) In TLE-MTS, thalamic volume loss is most prominent in the anterior thalamic and lateral dorsal nucleus, that is, nuclei receiving direct projections from CA1, the only hippocampal subfield with direct connections to the thalamus (Herkenham, 1978; Cenquizca & Swanson, 2006). Volume/neuronal loss there leads to loss of thalamocortical projections and thus to cortical thinning in the corresponding temporal and extratemporal projection areas. (2) Based on the assumption that the focus in TLE-no is located in the inferolateral temporal lobe, the medial pulvinar, which receives projections from this area, will show the most prominent volume loss. The distribution of extrafocal cortical thinning corresponds to cortical projection areas of the pulvinar.

Methods

Study population

The committees of human research at the University of California, San Francisco (UCSF); California Pacific Medical Center, San Francisco; and VA Medical Center, San Francisco approved the study, and written informed consent was obtained from each subject. Twenty-nine patients with drug-resistant TLE who agreed to participate in the 4T research protocol, which was administered in addition to the standard imaging procedures, were recruited between mid-2005 and the end of 2007 from the Pacific Epilepsy Program, California Pacific Medical Center, and the Northern California Comprehensive Epilepsy Center, UCSF, where they underwent evaluation for epilepsy surgery. Fifteen patients (mean age 41.3 ± 10.4 years, left TLE/right TLE 9/6, female/male 10/5) had evidence for mesiotemporal lobe sclerosis on their 1.5 T MR images (TLE-MTS) and 14 patients (mean age 39.8 ± 8.1 years, left TLE/right TLE 6/8, female/male 7/7) had normal-appearing hippocampi on their 1.5T MR images (TLE-no) and normal 1.5 T MR results. All the 1.5T reads were done by an experienced neuroradiologist. Hippocampal volumetry was used to confirm the presence (TLE-MTS) or absence (TLE-no)

of significant hippocampal volume loss on the 4T images. The identification of the epileptogenic focus was based on seizure semiology and prolonged ictal and interictal video/EEG/telemetry (VET) in all patients. The control population consisted of 29 healthy volunteers (mean age 37.7 ± 9.2 years, female/male 18/11). Table 1 displays the patient characteristics.

MRI acquisition

All imaging was performed on a Bruker MedSpec 4T system (Bruker MedSpec, Madison, WI, U.S.A.) controlled by a Siemens Trio (Siemens, Iselin, NJ, U.S.A.) console and equipped with a USA instruments (Aurora, OH, U.S.A.) eight-channel array coil. The following sequences were acquired: (1) for cortical thickness and thalamus measurements a volumetric T1-weighted gradient echo MRI (TR/TE/TI = 2,300/3/950 ms, 1.0 × 1.0 × 1.0 mm^3 resolution, acquisition time 5.17 min); (2) for the measurement of hippocampal subfields, a high-resolution T2-weighted fast-spin echo sequence (TR/TE: 3,500/19 ms, 0.4 × 0.4 mm in-plane, 2 mm slice thickness, 24 slices acquisition time 5:30 min); and (3) for the determination of the intracranial volume (ICV), a T2-weighted turbospin echo sequence (TR/TE 8,390/70 ms, 0.9 × 0.9 × 3 mm nominal resolution, 54 slices, acquisition time 3.06 min).

Cortical thickness measurement

All T_1 images were segmented using the expectation-maximization segmentation (EMS) algorithm (Van Leemput et al., 1999a,b). The bias field maps and tissue maps obtained from this process were used for bias correction and skull stripping of the T_1 image. To allow for a combination of left and right TLE in the analysis, the T_1 images of all patients with right TLE were side flipped so that the focus was on the left side in all patients. The same was done with all control images. FreeSurfer was used for cortical surface reconstruction and cortical thickness estimation of the original (controls and left TLE) and side-flipped (controls and right TLE) images. The procedure has been described extensively elsewhere (Dale et al., 1999; Fischl et al., 1999a,b; Desikan et al., 2006). All outputs underwent a quality check and were manually corrected if necessary (between 15 and 30 min/subject). A project-specific average spherical representation (average of original and side-flipped control data, original left TLE data, and side-flipped right TLE data) using a nonrigid high-resolution surface-based averaging method for an optimal alignment of the cortical folding pattern was generated. Each subjects' inflated brain was morphed onto this average for the vertex-based statistical analysis. The data were smoothed with a 20-mm full-width half-maximum (FWHM) Gaussian kernel to improve the signal-to-noise ratio. Mean cortical thickness in the ipsilateral inferior temporal gyrus (part of the presumed epileptogenic focus in TLE-no) (Vossler et al., 2004; Mueller et al., 2007a) for the correlation analyses was taken from the corresponding label of the FreeSurfer output. A region of interest (ROI) was manually drawn consisting of the regions in entorhinal cortex (ERC), parahippocampal gyrus, and lingual gyrus (ERC-paralingual ROI) in which cortical thickness was positively correlated with ipsilateral thalamic volume in TLE-MTS and controls, and TLE-no and controls (c.f. Fig. 1A) to identify the thalamic nuclei driving the overall thalamus volume loss.

Hippocampal subfield volumetry

The method used for subfield marking including assessment of measurement reliability has been described in detail previously (Mueller et al., 2007b). The marking scheme depends on anatomic landmarks, particularly on a hypointense line representing myelinated fibers in the stratum moleculare/lacunosum (Eriksson et al., 2008), which can be reliably visualized on these high-resolution images. Therefore, external and internal hippocampal landmarks are used to further subdivide the hippocampus into subiculum, cornu ammonis sectors (CA) CA1, CA1-2 transition zone, and CA3/dentate gyrus (c.f. Fig. 1B).

Thalamus deformation-based morphometry (DBM) and volumetry

An unbiased, symmetrical normal atlas was created from the original and side-flipped images of the control group. These images were coregistered (12 parameter affine) to a randomly selected nonflipped control image. Next, a fluid registration algorithm (Christensen et al., 1996) was used to generate the final symmetrical normal atlas using the technique described by Lorenzen et al. (2005) and Joshi et al. (2004). All images (original and side-flipped control images, original left TLE images, and side-flipped right TLE images) were then linearly coregistered to this symmetrical atlas (12 parameter affine). A 75 × 96 × 51 mm ROI centered on the thalamus was selected in the atlas, and in each image and the subject structures contained within this ROI were warped onto the corresponding structures in the atlas using a fluid registration algorithm (Christensen et al., 1996).

A deformation map for each subject was generated by calculating the jacobian determinant of the resulting nonlinear transformation matrix. The left and right thalamus region in each Jacobian map was identified and extracted from these deformation maps using thalamus labels obtained by manually marking both thalami in the atlas (see next paragraph) and smoothed with a 4-mm FWHM Gaussian spatial kernel for voxel-based statistical analysis. Because the normal atlas had been generated from the control population, a voxel expansion in patients compared to controls can be interpreted as evidence for volume loss in patients and a voxel contraction as volume gain.

The thalamus in the symmetrical atlas was manually traced using anatomic landmarks (Natsume et al., 2003). The so-obtained labels for the right and left thalamus were then applied to each subject's image by warping the thalamus region of the atlas onto the subject brain using a combination of linear and nonlinear coregistration steps. The resulting subject thalamus labels were visually inspected for accuracy and manually corrected if necessary. Figure 2B shows the manual thalamus tracing in the atlas and an example of the automatically obtained thalamus label in an individual subject.

Statistics

Thalamic side differences (left vs. right, and ipsi- vs. contralateral) were tested using a paired *t* test. After exclusion of side differences in the control group, left and right thalamus was averaged for the comparisons with TLE. Group differences between ipsi- and contralateral thalamus volumes were assessed using linear regression analysis followed by Tukey's post hoc tests. Thalamus volume was entered as dependent and "age," ICV, and "group" as independent measures. Regions of cortical thinning in TLE-MTS and TLE-no (side-flipped images for right TLE, original images for left TLE) compared to controls (original and side-flipped images) were tested for in a regionally unbiased way by computing a general linear model of the effect of "group" on thickness at each vertex using the statistical tool provided by FreeSurfer. A linear regression analysis was used to identify ipsilateral regions with significant correlations between ipsilateral thalamus volume (normalized to ICV because it had been shown to be highly dependent on ICV in the preliminary analysis) and cortical thickness (not a volume and hence not corrected for ICV) in controls and TLE-MTS and in controls and TLE-no. Age was used as a nuisance variable in these analyses because thalamus volume as well as cortical thickness had been found to be negatively correlated with age. False discovery rate (FDR) of $p \leq 0.05$ was applied to all FreeSurfer analyses to correct for multiple comparisons. SPM2 (Wellcome Department of Cognitive Neurology, http://www.fil.ion.ucl.ac.uk) running MATLAB 6.1 (The MathWorks, Natick, MA, U.S.A.) was used to search for differences between groups [TLE-MTS vs. controls, TLE-no versus controls, analysis of covariance (ANCOVA), age as nuisance variable, family-wise-error rate (FWR), $p \leq 0.05$ to correct for multiple comparisons] in the thalamus deformation maps. Partial correlation analyses with age as a nuisance variable were used to test for positive correlations

between regions of thalamic volume loss and ipsilateral CA1 volume, ipsilateral cortical thickness of the inferior temporal gyrus, and the ERC-paralingual ROI in controls and TLE-MTS and in controls and TLE-no.

Results

TLE-MTS

Thalamus volumetry and DBM—Table 2 displays the volumetric results. TLE-MTS had significantly smaller ipsi- and contralateral thalamus volumes than controls. There was no statistically significant difference between ipsi- and contralateral thalamus volumes (one-sided paired *t*-test $p = 0.07$). DBM showed regions of significant volume loss in the region of the ipsi- and contra-lateral anterior thalamic nucleus, the ipsilateral dorsal lateral nucleus, and ventral anterior nucleus extending toward the ventral lateral nucleus and posterior lateral nucleus. A smaller region of significant volume loss was found in the medial pulvinar (c.f. Fig. 3B).

Cortical thickness and correlations with thalamus volume/DBM—Compared to controls TLE-MTS had regions of significant extensive cortical thinning in the ipsilateral temporal medial region (entorhinal, parahippocampal, fusiform gyrus), medial and lateral prestriate regions (lingual gyrus, lateral occipital gyrus, superior parietal), and in the posterior cingulate. Smaller regions were found temporal lateral (medial, superior temporal gyrus), pre/postcentral, and frontal dorsal (superior frontal gyrus) (c.f. Fig. 3A). The ipsilateral thalamus volume was positively correlated with cortical thickness in the entorhinal/parahippocampal and lingual region and with smaller regions in the superior parietal region and superior temporal gyrus, that is, regions that showed also significant thinning in the group comparison (c.f. Fig. 4A).

In the next step, we tested for a significant positive correlation of the ipsilateral CA1 volume and mean thickness of the ROI encompassing the regions in the ERC-paralingual ROI and inferior temporal gyrus with volume loss within the ipsilateral thalamus. CA1 volume was positively correlated with thalamic volume loss in a region encompassing the anterior thalamic and dorsal medial nucleus and expanding toward the medial part of the lateral ventral nucleus (c.f. Fig. 4B). Mean thickness in the ERC-paralingual ROI was positively correlated with volume loss in the anterior thalamic nucleus, lateral dorsal nucleus, middle dorsal nucleus, ventral nucleus, and pulvinar (c.f. Fig. 4C). There was no such correlation for mean thickness of the inferior temporal gyrus.

TLE-no

Thalamus volumetry and DBM—Thalamic volumes of TLE-no were between the volumes of controls and TLE-MTS but were not significantly different from either, and there was no significant side difference between ipsi- and contralateral thalamus volumes (one-sided paired *t*-test $p = 0.20$). DBM showed no significant difference between TLE-no and controls. In order to answer the question if the mild thalamic volume loss in TLE-no affects similar regions as in TLE-MTS, the threshold for significance was lowered [$p \leq 0.005$, no correction for multiple comparisons (cmc)]. Using this less-restrictive threshold, the group comparison showed a circumscribed volume loss in the ipsilateral dorsal lateral nucleus in TLE-no (c.f. Fig. 5B).

Cortical thickness and correlations with thalamus volume/DBM—Compared to controls, TLE-no showed significant cortical thinning in the ipsilateral inferior and lateral temporal lobe (inferior, medial, and superior temporal gyrus), insula and operculum, pre/postcentral gyrus, dorsal and medial superior frontal gyrus, and lateral orbito-frontal. Smaller regions were also found in the prestriatal region (c.f. Fig. 5A). There were no significant

correlations between ipsilateral thalamus volume and ipsilateral cortical thickness. If the threshold for significance was lowered ($p \leq 0.005$, no cmc), there was a positive correlation between thalamus volume and cortical thickness in ERC, parahippocampal gyrus, lingual gyrus, and a smaller region in the lateral occipital cortex (c.f. Fig. 6A.)

When testing for correlations ($p \leq 0.005$, no cmc) between thalamus volume loss and mean thickness in ipsilateral ERC-paralingual ROI, mean inferior temporal gyrus thickness, and CA1 volume, thickness in the ERC-paralingual ROI was correlated with volume loss in the anterior thalamic nucleus, lateral and middle dorsal nucleus, and ventral nucleus and pulvinar (c.f. Fig. 6B), and inferior temporal gyrus thickness was correlated with volume loss in the region of the anterior thalamic nucleus (c.f. Fig. 6C). There was no correlation between CA1 volume and thalamic volume loss.

Discussion

There were two major findings in this study: (1) In TLE-MTS thalamic volume loss was most prominent in the anterior thalamus and correlated with volume loss/cortical thinning in mesiotemporal regions with known reciprocal connections to these nuclei. Although TLE-MTS showed extensive extratemporal cortical thinning in comparison with controls, thinning in these regions was not correlated with thalamic volume loss. (2) Thalamic volume loss in TLE-no was less extensive than in TLE-MTS and also located in the anterior thalamus. The thalamic volume was correlated with cortical thickness in the mesiotemporal region. Similarly as TLE-MTS, TLE-no had widespread extratemporal cortical thinning but this was not correlated with thalamus volume. These findings suggest that the thalamus has a similar role in TLE-MTS and TLE-no, that is, in both TLE types seizures spread from the epileptogenic focus or a region close to the focus in the temporal lobe to the thalamus. This results in a correlation between the thinning/volume loss in the epileptogenic focus with the volume loss in the corresponding thalamic projection regions. However, the fact that the volume loss in the thalamus was mostly not correlated with extratemporal cortical thinning in TLE-MTS or in TLE-no suggests that deafferentation of thalamocortical projections or local excitotoxic effects of seizure propagation via the thalamus into other cortical regions are not responsible for the widespread extrafocal cortical abnormalities seen in TLE.

TLE-MTS: Thalamotemporal correlations

The first major finding was that TLE-MTS had bilateral thalamic volume loss, which was most prominent in a region encompassing the ipsilateral anterior thalamic nucleus, dorsal lateral nucleus, and ventral anterior nucleus. The volume loss in these nuclei also correlated with volume loss in the ipsilateral CA1, which has dense reciprocal projections to them (Herkenham, 1978; McKenna & Vertes, 2004; Saunders et al., 2005; Cenquizca & Swanson, 2006). This finding is consistent with the assumption that neuronal loss in the presumed focus, that is, hippocampus, results in neuronal loss in thalamic projection regions, either by deafferentation or by local excitotoxic effects of the spreading epileptic activity. Ipsilateral thalamus volume loss located by DBM in the anterior thalamic, lateral and middle dorsal nucleus, ventral anterior nucleus, and parts of the pulvinar, was correlated with cortical thickness in the ERC and parahippocampal and lingual gyrus, which are known to project to these thalamic nuclei (Saunders et al., 2005). ERC and parahippocampal gyrus, which are either part of the primary epileptogenic zone in the mesial temporal lobe or closely connected to it, showed also thinning in the direct comparison between TLE-MTS and controls. This indicates that neuron loss in the hippocampus and/or mesiotemporal cortical regions closely connected to it could contribute to the neuronal loss observed in the thalamus in TLE-MTS.

TLE-MTS: Thalamo-extratemporal correlations

The relationship between thalamic volume loss and extra-focal or extratemporal structural abnormalities in TLE-MTS is more complex. On the one hand, thalamus volume was correlated with cortical thickness in circumscribed regions within the superior temporal gyrus and superior parietal lobe. These regions showed also extensive thinning in the direct comparison of TLE-MTS with controls. Both cortical regions receive thalamic input from the pulvinar and posterior lateral nucleus (Taktakishvili et al., 2002; Rosenberg et al., 2009), which showed mild volume loss in the direct comparison of TLE-MTS with controls. These findings suggest that seizure propagation (Guye et al., 2006; Rosenberg et al., 2006) between pulvinar/posterior lateral nucleus and parietal/temporal regions might at least partially be responsible for the cortical thinning observed in these regions. On the other hand, the anterior thalamic nucleus, lateral dorsal nucleus, and ventral anterior nucleus, that is, the nuclei with the most prominent volume loss, have extratemporal projections to the anterior, posterior, and retrosplenial cingulate and the prefrontal cortex (Groenewegen et al., 1997; Hoover & Vertes, 2007). Thinning in these regions, if present at all, was not correlated with thalamic volume. This suggests that the epileptogenic activity either spreads into these regions by other, nonthalamic pathways or that seizure spread by the thalamic pathway does not result in neuronal loss in these cortical projection areas. Interestingly, this latter possibility is supported by a recent study in rats, which showed neuronal loss in CA1 and thalamic midline nuclei after kainate-induced status epilepticus. Although this was associated with functional abnormalities in the prefrontal projection areas of these midline nuclei, there was no evidence for neuronal loss in these regions in the histopathologic analysis (Sloan & Bertram, 2008). Alternatively, it is also possible that the extrafocal cortical thinning is not a consequence of the epileptogenic activity but rather the cause of it, for example, that regions of thinning represent regions with subtle epileptogenic cortical malformations, for example, microdysgenesis (Bothwell et al., 2001; Thom et al., 2001).

TLE-no: Thalamotemporal correlations

The second major finding was that TLE-no had bilaterally smaller thalami than controls, although the difference was not significant. After lowering the threshold of significance, the most prominent volume loss in comparison with controls was found in the region of the dorsal lateral nucleus. The thalamic volume correlated with cortical thickness in the ERC/parahippocampal and lingual gyrus region, and DBM showed a significant correlation between thickness in these regions and volume loss in the anterior thalamic, lateral dorsal, middle dorsal, ventral anterior nucleus, and pulvinar (Saunders et al., 2005). So far the findings in TLE-no are reminiscent of those in TLE-MTS, although the volume losses were generally milder than in TLE-MTS. However, in contrast to TLE-MTS, CA1 volume in TLE-no was not correlated with volume loss in the anterior thalamic/dorsal lateral nucleus. Furthermore, the thickness in the inferior temporal gyrus correlated with volume loss in the anterior thalamic nucleus, despite the fact that this nucleus receives only indirect projections (via the ERC/parahippocampus (Martin-Elkins & Horel, 1992) from the inferior temporal gyrus. These findings suggest that in TLE-no seizure propagation directly from the focus into the thalamus either does not occur or does not result in thalamic neuronal loss detectable by the methods used in this study. An alternative explanation is that seizure spread from the focus to the thalamus occurs indirectly via the ERC/parahippocampal region.

TLE-no: Thalamo-extratemporal correlations

TLE-no displayed extensive temporal and extratemporal cortical thinning compared to controls. The distribution of these regions showed a good overlap with known cortical projection areas of the anterior thalamic, the ventral anterior nucleus, and the pulvinar. However, the thinning in these regions was not correlated with the thalamic volume and in

contrast to the prominent cortical thinning, these nuclei showed only mild volume loss. Therefore, thalamic neuronal loss with consecutive deafferentation and neuronal loss in cortical projection areas are unlikely to explain the temporal and extratemporal thinning as are local excitotoxic effects of seizure propagation, which spare the thalamus but affect cortical regions (Margerison & Corsellis, 1966; Lothman & Collins, 1981; Willoughby et al., 1997; Sloan & Bertram, 2008). Taken together, the findings suggest that in TLE-no seizures propagate into the thalamus and cause neuronal loss in circumscribed thalamic regions similar to that in TLE-MTS. The pattern of volume loss suggests that the thalamic spread occurs indirectly via the ERC/parahippocampal region. The fact that the thalamic volume loss is not correlated with extratemporal thinning suggests that the extensive extratemporal structural abnormalities in TLE-no cannot be explained by deafferentation of thalamic projections or local excitotoxic effects of seizure propagation via the thalamus. Similar mechanisms as discussed for TLE-MTS could also be responsible for the cortical thinning in TLE-no.

The study has limitations. (1) The sample sizes of TLE-MTS and TLE-no is small and, therefore, patients with left and right-sided TLE were pooled for the analysis. Although we tried to correct for this by using original and side-flipped images of controls for cortical thickness assessments and by generating a symmetrical unbiased population atlas for DBM and for the generation of the thalamus masks, we cannot exclude that we introduced additional noise into the analysis and thus missed some of the more subtle effects. Therefore, these results have to be considered as preliminary and need to be validated in a larger dataset, ideally in combination with diffusion tensor imaging to assess the integrity of the corresponding white matter tracts. (2) It would be desirable to corroborate the presumed seizure origin in the two patient groups, that is, hippocampal in TLE-MTS and inferolateral temporal in TLE-no, and the different thalamic involvement by depth EEG recordings. However, only a subset of patients in this population has undergone invasive EEG, and stereotactic exploration of the thalamus is not a routine procedure in these cases. (3) All patients were recruited from tertiary epilepsy centers where they were referred for presurgical exploration and thus are likely to have a more severe form of TLE. Therefore, the findings in this study might not be applicable to TLE in general.

In conclusion, our findings suggest that that seizure propagation into the thalamus from the presumed epileptogenic focus or regions close to it occurs in TLE-MTS and TLE-no and results in circumscribed neuronal loss in thalamic nuclei connected to these regions. However, although these nuclei have projections onto other cortical areas, seizure spread beyond the thalamus with consecutive cortical deafferentation or local excitotoxic effects is unlikely to explain the widespread extratemporal structural abnormalities in TLE. This suggests that seizure spread by other cortical networks might be responsible for the widespread extratemporal structural abnormalities in TLE.

Acknowledgments

This work was supported by the National Institutes of Health (RO1-NS31966 to K.D.L.). We confirm that we have read the Journal's position on issues involved in ethical publication and affirm that this report is consistent with those guidelines.

References

Bertram EH, Zhang DX, Williamson JM. Multiple roles of midline dorsal thalamic nuclei in induction and spread of limbic seizures. Epilepsia 2008;49:256–268. [PubMed: 18028408]

Bothwell S, Meredith GE, Phillips J, Staunton H, Doherty C, Grigorenko E, O'Donovan CA, Farrell M. Neuronal Hypertrophy in the neocortex of patients with temporal lobe epilepsy. J Neurosci 2001;21:4789–4800. [PubMed: 11425906]

Carne RP, Cook MJ, MacGregor LR, Kilpatrick CJ, Hicks RJ, O'Brien TJ. Magnetic resonance imaging negative positron emission tomography positive temporal lobe epilepsy: FDG-PET pattern differs from mesial temporal lobe epilepsy. Mol Imaging Biol 2007;9:32–42. [PubMed: 17176980]

Cassidy RM, Gale K. Mediodorsal thalamus plays a critical role in the development of limbic motor seizures. J Neurosci 1998;18:9002–9009. [PubMed: 9787005]

Cenquizca LA, Swanson LW. Analysis of direct hippocampal cortical field CA1 axonal projections to diencephalon in the rat. J Comp Neurol 2006;497:101–114. [PubMed: 16680763]

Christensen GE, Rabbitt RD, Miller MI. Deformable templates using large deformation kinematics. IEEE Trans Image Process 1996;5:1435–1447. [PubMed: 18290061]

Dale AM, Fischl B, Sereno MI. Cortical surface-based analysis I: segmentation and surface reconstruction. Neuroimage 1999;9:179–194. [PubMed: 9931268]

Desikan RS, Ségonne F, Fischl B, Quinn BT, Dickerson BC, Blacker D, Buckner RL, Dale AM, Maguire RP, Hyman BT, Albert MS, Killiany RJ. An automated labeling system for subdividing the human cerebral cortex on MRI scans into gyral based regions of interest. Neuroimage 2006;31:968–980. [PubMed: 16530430]

Eriksson SH, Thom M, Bartlett P, Symms MR, McEvoy AW, Sisodiya SM, Duncan JS. PROPELLER MRI visualizes detailed pathology of hippocampal sclerosis. Epilepsia 2008;49:33–39. [PubMed: 17877734]

Fischl B, Sereno MI, Dale AM. Cortical surface-based analysis. II: inflation, flattening, and a surface-based coordinate system. Neuroimage 1999a;2:195–207.

Fischl B, Sereno MI, Tootell RB, Dale AM. High-resolution inter-subject averaging and a coordinate system for the cortical surface. Hum Brain Mapp 1999b;8:272–284. [PubMed: 10619420]

Gong G, Concha L, Beaulieu C, Gross DW. Thalamic diffusion and volumetry in temporal lobe epilepsy with and without mesial temporal sclerosis. Epilepsy Res 2008;80:184–193. [PubMed: 18490143]

Groenewegen HJ, Wright CI, Uylings HBM. The anatomical relationships of the prefrontal cortex with limbic structures and the basal ganglia. J Psychopharmacol 1997;11:99–106. [PubMed: 9208373]

Guye M, Régis J, Tamura M, Wendling F, Mc Gonigal A, Chauvel P, Bartolomei F. The role of corticothalamic coupling in human temporal epilepsy. Brain 2006;129:1917–1928. [PubMed: 16760199]

Herkenham M. The connections of the nucleus reuniens thalami: evidence for a direct thalamo-hippocampal pathway in the rat. J Comp Neurol 1978;177:589–610. [PubMed: 624792]

Hoover WB, Vertes RP. Anatomical analysis of afferent projections to the medial prefrontal cortex in the rat. Brain Struct Funct 2007;212:149–179. [PubMed: 17717690]

Joshi S, Davis B, Jomier M, Gerig G. Unbiased diffeomorphic atlas construction for computational anatomy. Neuroimage 2004;23(suppl 1):S151–S160. [PubMed: 15501084]

Juhasz C, Nagy F, Watson C, da Silva EA, Muzik O, Chugani DC, Shah J, Chugani HT. Glucose and [11C]flumazenil positron emission tomography abnormalities of thalamic nuclei in temporal lobe epilepsy. Neurology 1999;53:2037–2045. [PubMed: 10599778]

Jutila L, Ylinen A, Partanen K, Alafuzoff I, Mervaala E, Partanen J, Vapalathi M, Vaino P, Pitkanen A. MR volumetry of the entorhinal, perirhinal and temporopolar cortices in drug refractory temporal lobe epilepsy. AJNR Am J Neuroradiol 2001;22:1490–1501. [PubMed: 11559496]

Keller SS, Wilke M, Wieshmann UC, Sluming VA, Roberts N. Comparison of standard and optimized voxel-based morphometry for analysis of brain changes associated with temporal lobe epilepsy. Neuroimage 2004;23:860–868. [PubMed: 15528086]

Labate A, Cerasa A, Gambardella A, Aguglia U, Quattrone A. Hippocampal and thalamic atrophy in mild temporal lobe epilepsy. A VBM study. Neurology 2008;7:1094–1101. [PubMed: 18824674]

Lorenzen P, Davis B, Joshi S. Unbiased atlas formation via large deformation metric mapping. Med Image Comput Comput Assist Interv Int Med Image Comput Comput Assist Interv 2005;8:411–418.

Lothman EW, Collins RC. Kainic acid induced limbic seizures: metabolic, behavioral, electroencephalographic and neuropathological correlates. Brain Res 1981;218:299–318. [PubMed: 7272738]

Margerison JH, Corsellis JAN. Epilepsy and the temporal lobes. A clinical, electroencephalographic and neuropathological study of the brain in epilepsy, with particular reference to the temporal lobes. Brain 1966;89:499–530. [PubMed: 5922048]

Martin-Elkins CL, Horel JA. Cortical afferents to behaviorally defined regions of the inferior temporal and parahippocampal gyri as demonstrated by WGA-HRP. J Comp Neurol 1992;321:177–192. [PubMed: 1380012]

McKenna JT, Vertes RP. Afferent projections to nucleus reuniens of the thalamus. J Comp Neurol 2004;480:115–142. [PubMed: 15514932]

Moran NE, Lemieux L, Kitchen ND, Fish DR, Shorvon SD. Extra-hippocampal temporal lobe atrophy in temporal lobe epilepsy and mesial temporal sclerosis. Brain 2001;124:167–175. [PubMed: 11133796]

Mueller SG, Laxer KD, Cashdoller N, Buckley S, Paul C, Weiner MW. Voxel-based optimized morphometry (VBM) of gray and white matter in temporal lobe epilepsy (TLE) with and without mesial temporal sclerosis. Epilepsia 2006;47:900–907. [PubMed: 16686655]

Mueller SG, Laxer KD, Schuff N, Weiner MW. Voxel-based T2 relaxation rate measurements in temporal lobe epilepsy (TLE) with and without mesial temporal sclerosis. Epilepsia 2007a;48:220–280. [PubMed: 17295614]

Mueller SG, Stables L, Du AT, Schuff N, Truran D, Cashdollar N, Weiner MW. Measurement of hippocampal subfields and age-related changes with high resolution MRI at 4T. Neurobiol Aging 2007b;28:719–726. [PubMed: 16713659]

Natsume J, Bernasconi N, Andermann F, Bernasconi A. MRI volumetry of the thalamus in temporal, extratemporal, and idiopathic generalized epilepsy. Neurology 2003;60:1296–1300. [PubMed: 12707432]

Rosenberg DS, Mauguière F, Demarquay G, Ryvlin P, Ismard J, Fischer C, Guénot M, Magnin M. Involvement of medial pulvinar thalamic nucleus in human temporal lobe seizure. Epilepsia 2006;47:98–107. [PubMed: 16417537]

Rosenberg DS, Mauguiere F, Catenoix H, Faillenot I, Magnin M. Reciprocal thalamocortical connectivity of the medial pulvinar: a depth stimulation and evoked potential study in human brain. Cereb Cortex 2009;19:1462–1473. [PubMed: 18936272]

Saunders RC, Mishkin M, Aggleton JP. Projections from the entorhinal cortex, perirhinal cortex, presubiculum, and parasubiculum to the medial thalamus in macaque monkeys: identifying different pathways using disconnection techniques. Exp Brain Res 2005;167:1–16. [PubMed: 16143859]

Seidenberg M, Herman B, Pulsipher D, Morton J, Parrish J, Geary E, Guidotti L. Thalamic atrophy and cognition in unilateral temporal lobe epilepsy. J Int Neuropsychol Soc 2008;14:384–393. [PubMed: 18419837]

Sloan DM, Bertram EH. Changes in midline thalamic recruiting responses in the prefrontal cortex of the rat during the development of the chronic limbic seizures. Epilepsia 2008;1:1–10.

Taktakishvili O, Sivan-Loukianova E, Kultas-Ilinsky K, Ilinsky IA. Posterior parietal cortex projections to the ventral lateral and some association thalamic nuclei Macaca mulatta. Brain Res Bull 2002;59:135–150. [PubMed: 12379444]

Thom M, Sisodiya S, Harkness W, Scaravilli F. Microdysgenesis in temporal lobe epilepsy. A quantitative and immunohistological study of white matter neurons. Brain 2001;124:2299–2309. [PubMed: 11673330]

Van Leemput K, Maes F, Vandermeulen D, Suetens P. Automated model-based bias field correction of MR images of the brain. IEEE Trans Med Imaging 1999a;18:885–896. [PubMed: 10628948]

Van Leemput K, Maes F, Vandermeulen D, Suetens P. Automated model-based tissue classification of MR images of the brain. IEEE Trans Med Imaging 1999b;18:897–908. [PubMed: 10628949]

Vossler DG, Kraemer DL, Haltiner AM, Rostad SW, Kjos BO, Davis BJ, Morgan JD, Caylor LM. Intracranial EEG in temporal lobe epilepsy: location of seizure onset relates to degree of hippocampal pathology. Epilepsia 2004;45:497–503. [PubMed: 15101831]

Willouoghby JO, Mackenzie L, Medvedev A, Hiscock JJ. Fos induction following systemic kanic acid: early expression in hippocampus and later widespread expression correlated with seizure. Neuroscience 1997;77:379–392. [PubMed: 9472398]

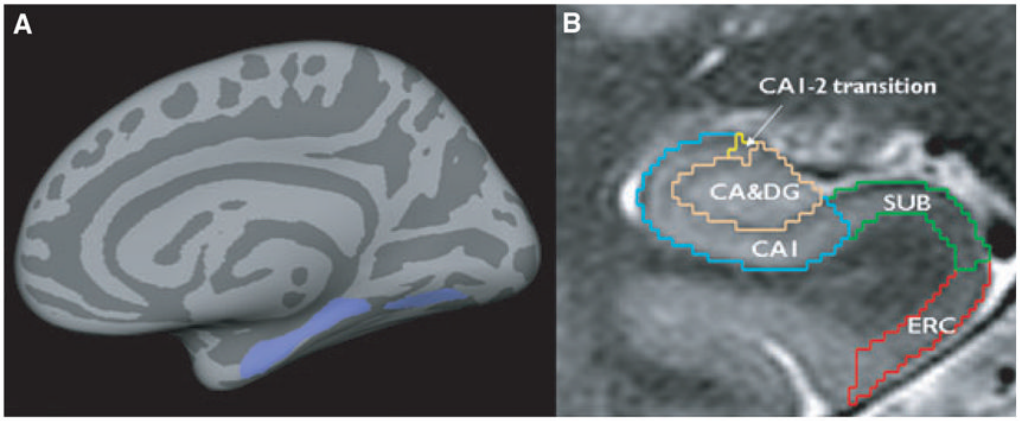

Figure 1.

(**A**) Region of interest (ROI, lilac) containing parts of the ERC, parahippocampal, and lingual gyrus (ERC-paralingual ROI). Size and shape of the ROI were based on the region that showed significant correlations with the total ipsilateral thalamus volume in TLE-no and controls. (**B**) Manual marking scheme for hippocampal subfields. As it is not possible to identify individual hippocampal layers with 4T, the scheme was based on reliably recognizable anatomic landmarks, even though this resulted in a part of the prosubiculum and subiculum proper being counted toward the CA1 sector. ERC, entorhinal cortex; CA1-2, CA1-CA2 transition zone. Subfields were marked in the anterior part of the hippocampal body on a length of 1 cm, c.f. references in text for a detailed explanation of the marking scheme.

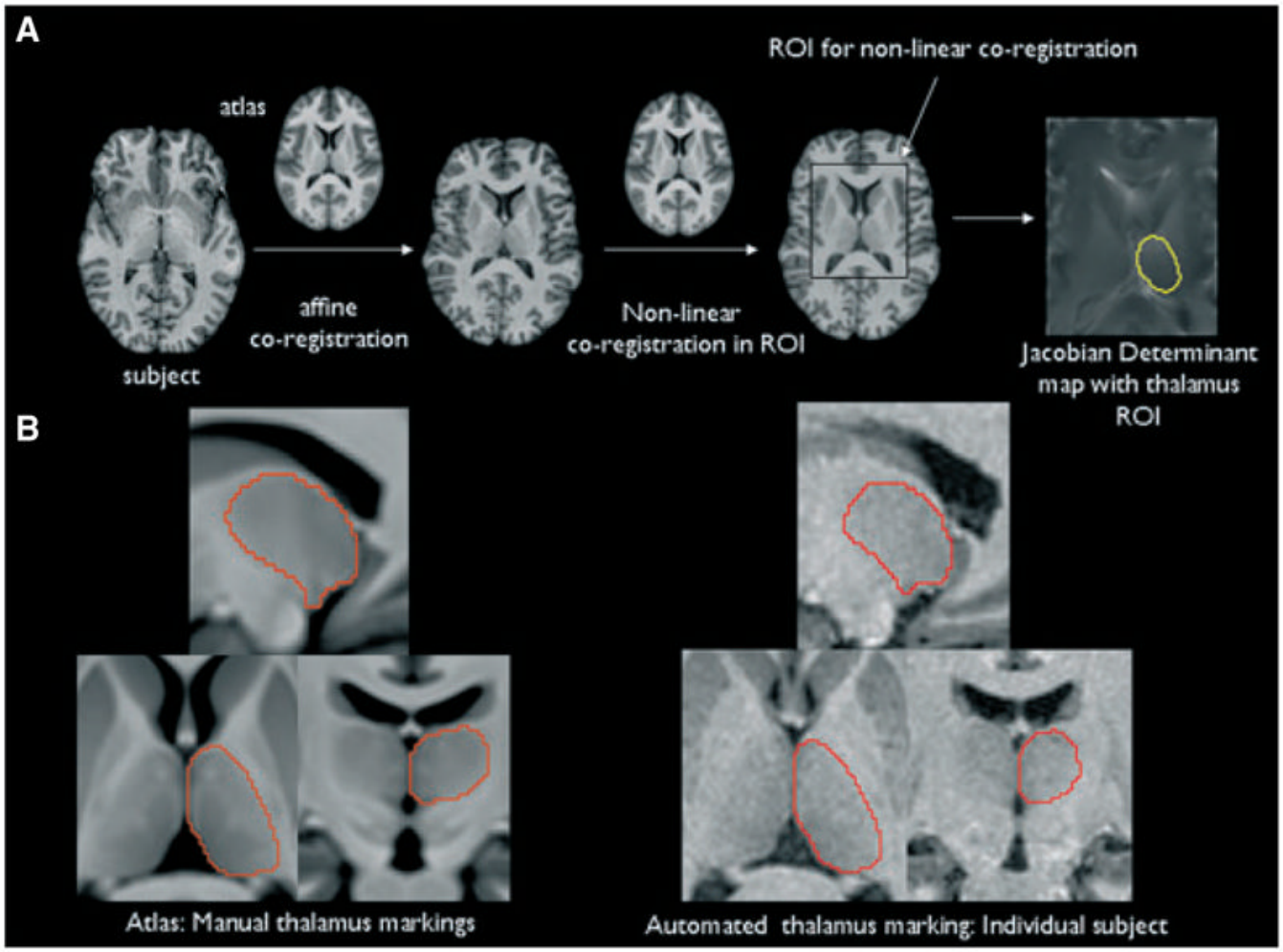

Figure 2.

(**A**) Overview of the generation of the thalamus deformation map. The yellow region in the right-most image indicates the left-sided thalamus label that was used to select the thalamus. (**B**) Left side: Atlas with manual thalamus tracings. The enhanced contrast of the atlas allows one to distinguish details of the internal structure, including some of the major nuclei of the thalamus. Right side: Automated thalamus tracings in an individual subject. Please refer to the text for details.

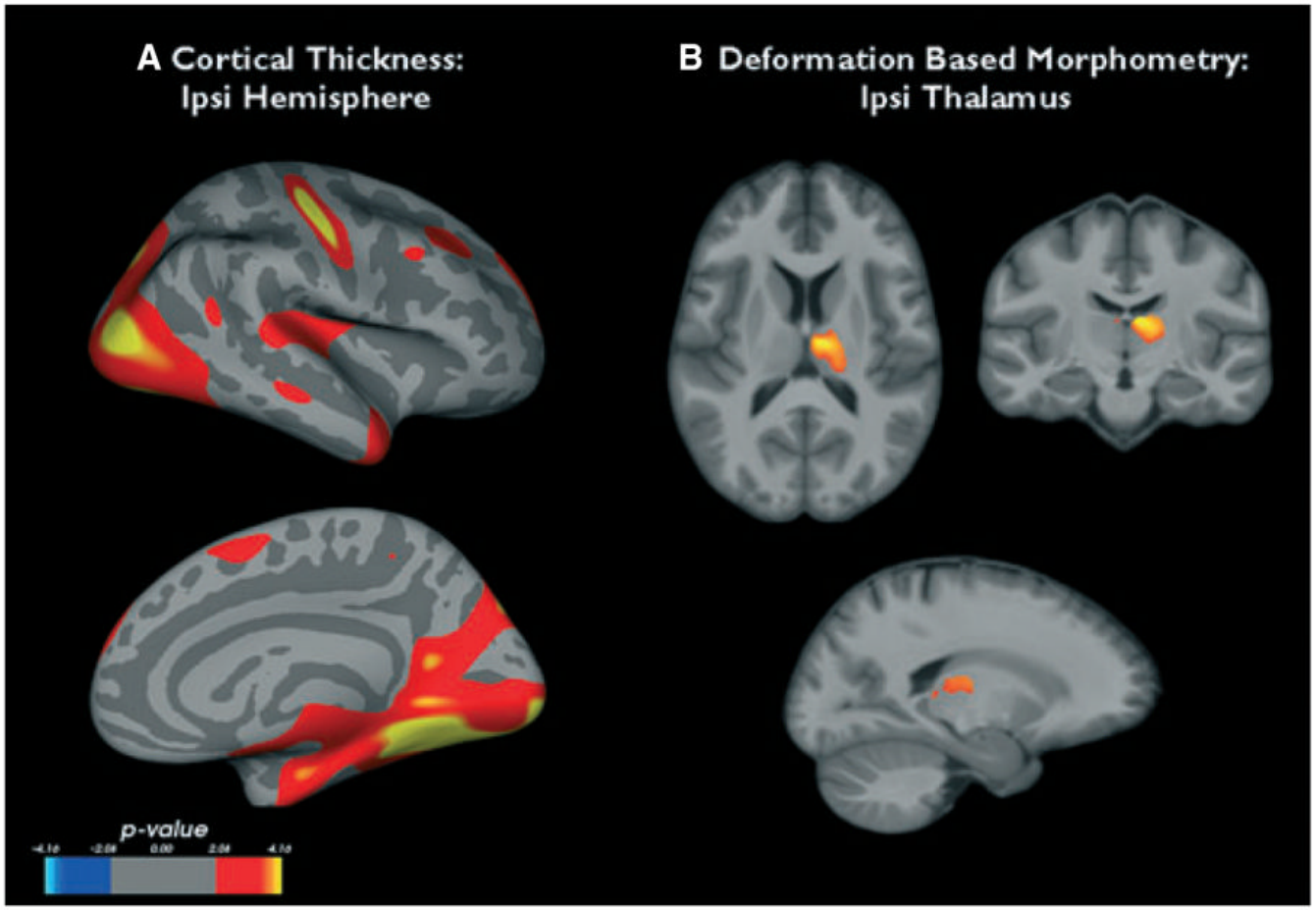

Figure 3.
(**A**) Regions of cortical thinning in the ipsilateral hemisphere of temporal lobe epilepsy with mesiotemporal sclerosis (TLE-MTS) compared to the control group. (**B**) Thalamic regions showing significant volume loss in TLE-MTS compared to controls. See text for statistical thresholds.
Epilepsia © ILAE

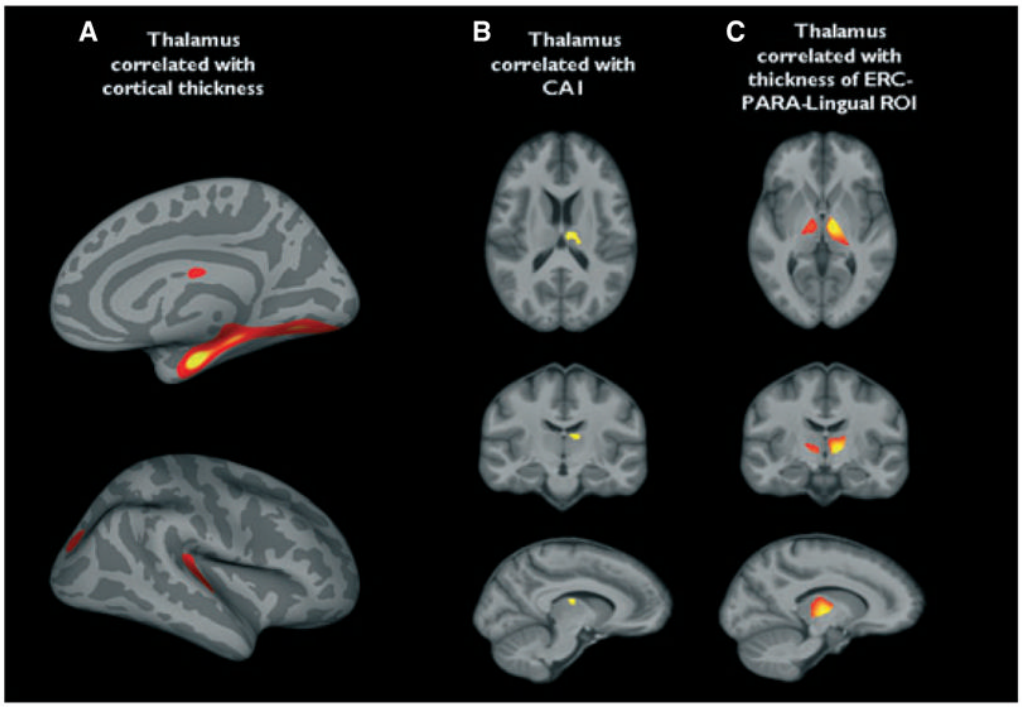

Figure 4.

(**A**) Regions in which there is a statistically significant positive correlation of cortical thickness with ipsilateral total thalamus volume in temporal lobe epilepsy with mesiotemporal sclerosis (TLE-MTS) and controls (false detection rate, $p \leq 0.05$). Regions of thalamic volume loss, which were significantly correlated with (**B**) CA1 volume. (**C**) Mean thickness of the entorhinal cortex (ERC)-paralingual region of interest (ROI). Correction for multiple comparisons [family-wise-error rate (FWR), $p \leq 0.05$].

Epilepsia © ILAE

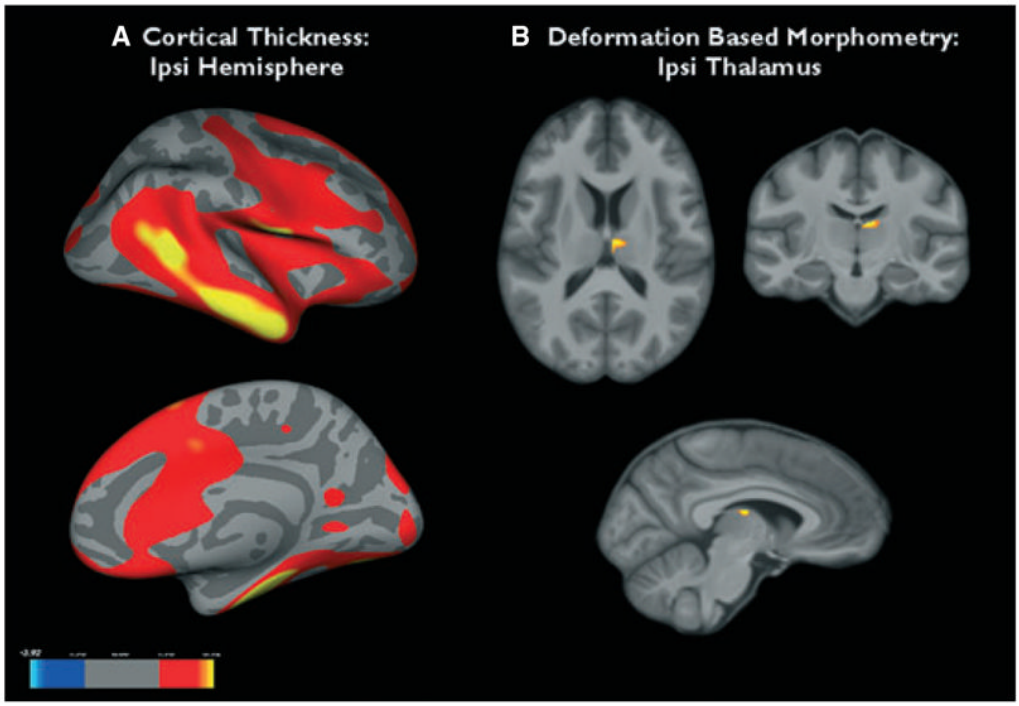

Figure 5.
(**A**) Regions of cortical thinning in the ipsilateral hemisphere of temporal lobe epilepsy (TLE)-no compared to the control group. (**B**) Thalamic regions that showed volume loss in TLE-no compared to controls. See text for statistical thresholds.
Epilepsia © ILAE

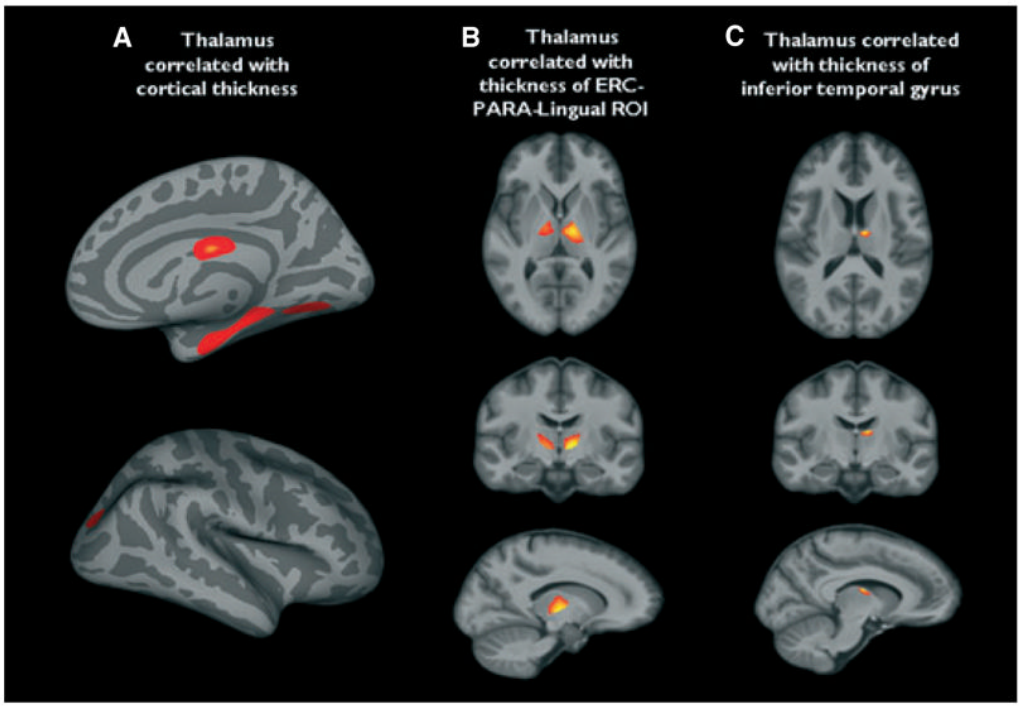

Figure 6.

(**A**) Regions in which there is a statistically significant positive correlation of cortical thickness with ipsilateral thalamus volume in temporal lobe epilepsy (TLE)-no and controls. (**B**) Regions of ipsilateral thalamic volume loss in this group that are positively correlated with thickness of the entorhinal cortex (ERC)-paralingual region of interest (ROI). (**C**) Regions of thalamic volume loss that were significantly correlated with (**A**). Mean thickness of the interior temporal gyrus and (c.f. Fig. 6C). A threshold of $p \leq 0.005$ without correction for multiple comparisons was used for all analyses (Fig. 6A–C).

Epilepsia © ILAE

Epilepsia. Author manuscript; available in PMC 2010 October 6.

Table 1

Patient characteristics

Patient no.	Age (year)	Gender	Ictal VET	Precipitating events/risk factors	Age at onset of seizures	1.5 T Clinical MRI	Surgery/histology/outcome
1	46	Male	L temp	No	3	L MTS	Yes/MTS/I
2	35	Male	L temp	No	2	L MTS	Yes/MTS/I
3	50	Female	L temp	Febrile seizure	2	LMTS	Yes/MTS/I
4	24	Female	L temp	No	13	LMTS	Yes/MTS/I
5	35	Female	L temp	No	9	LMTS	Yes/MTS/II
6	54	Male	L temp	No	50	LMTS	No
7	44	Male	L temp	No	28	LMTS	Yes/na*/III
8	48	Female	L temp	No	13	BilMTS	No
9	38	Female	L temp	Febrile seizure	6	BilMTS	No
10	46	Female	R temp	Posttraumatic	6	RMTS	No
11	28	Female	R temp	Febrile seizure	13	RMTS	Yes/MTS/I
12	49	Female	R temp	No	7	RMTS	Yes/MTS/I
13	23	Female	R temp	Infection	6	RMTS	na
14	43	Male	R temp	No	5	RMTS	Yes/MTS/I
15	56	Female	R temp	No	12	RMTS	No
16	27	Female	L temp	No	10	Normal	Mo
17	33	Female	L temp	No	10	Normal	No
18	35	Female	L temp	No	32	Normal	No
19	42	Female	L temp	No	21	Normal	No
20	38	Female	L temp	Posttraumatic	37	Normal	No
21	51	Male	L temp	No	18	Normal	No
22	29	Male	R temp	No	11	Normal	Yes/norm/I
23	43	Female	R temp	Birth complications	20	Normal	No
24	45	Female	R temp	No	31	Normal	No
25	33	Male	R temp	No	23	Normal	Yes/norm/I
26	45	Male	R temp	Posttraumatic	30	Normal	Yes/norm/I
27	39	Male	R temp	No	13	Normal	Yes/norm/I
28	56	Male	R temp	Posttraumatic	49	Normal	No
29	41	Male	R temp	Posttraumatic	40	Normal	No

R, right; L, left; temp, temporal; MTS, mesiotemporal sclerosis; norm, no MTS in histology; No, none; posttraumatic, mild closed head trauma (concussion wo. structural defect) in history without temporal relationship to onset of seizures; infection, history of meningitis or encephalitis; na*, no histology, gamma knife surgery.

Table 2

Volumes/thickness of the regions of interest

Group	Side	Thalamus (cm^3)	CA1 (mm^2)	ERC-parahippocampus-lingual ROI (mm)
Control	Left	6.0 (0.6)	179.2 (22.1)	2.55 (0.16)
	Right	6.1 (0.6)	175.9 (23.2)	2.59 (0.15)
TLE-MTS	Ipsi	5.2 (0.6)[a]	101.1 (23.3)[a]	2.35 (0.20)[a]
	Contra	5.3 (0.7)[a]	166.6 (35.1)	na
TLE-no	Ipsi	5.8 (0.6)	177.4 (19.3)	2.45 (0.18)
	Contra	5.7 (0.5)	175.0 (26.4)	na

[a] Smaller $p < 0.05$ compared to controls, numbers in brackets are standard deviations.

ERC-parahippocampus-lingual ROI, entorhinal-parahippocampus-lingual region of interest.

Thalamus and CA1 volumes are normalized for head size using the formula: normalized volume = raw volume * 1,000 cm^3/intracranial volume in cm^3